

Direct transfer reaction to discrete and continuum states

M. C. Mermaz

DPh-N/BE, CEN Saclay, BP 2, 91190 Gif-sur-Yvette, France

(Received 8 October 1979)

A parametrization based on the distorted-wave Born-approximation (DWBA) formalism, using the diffractive model, is given in order to fit angular distributions and continuum energy spectra of direct transfer reactions induced by heavy ions populating continuum states at incident energy well above the Coulomb barrier. Experimental data analysis of two-proton and alpha-transfer reactions on 1f-2p shell nuclei are successful at low incident energies. On the other hand, at high incident energy, alpha stripping induced by ¹⁶O beam on ²⁰⁸Pb cannot be described by this direct surface reaction model. It turns out that fragmentation is the most likely process.

NUCLEAR REACTIONS DWBA and diffractive model applied to direct reactions induced by heavy ions—continuum states. Analysis of ⁵⁴Fe(¹⁶O, ¹²C)⁵⁸Ni, ⁴⁸Ca(¹⁶O, ¹⁴C)⁵⁰Ti, ⁶⁴Ni(¹⁶O, ¹⁴C)⁶⁶Zn, ⁷⁶Ge(¹⁶O, ¹⁴C)⁷⁸Se, ²⁰⁸Pb(¹⁶O, ¹⁵N)²⁰⁹Bi, ²⁰⁸Pb(¹⁶O, ¹²C)²¹²Po, and ²⁰⁸Pb(¹⁶O, ¹¹B)²¹³At reactions.

I. INTRODUCTION

The populations of the first few discrete levels in heavy ion transfer reactions are rather well described by the distorted wave method formalisms such as the distorted wave Born approximation (DWBA) and/or the coupled channel Born approximation (CCBA) for two-step processes involving core excitation of target and residual nucleus and/or projectile-ejectile system.¹

Furthermore, for heavy ion reactions occurring well above the Coulomb barrier, continuum states are also strongly populated and some authors, using the previous formalism used for discrete transitions, but with large simplifications, have already succeeded in explaining the energy spectra as well as the angular distributions of the continuum states.²

We want to present here a similar but more simple model assuming that the reactions proceed mainly by one-step processes. The DWBA transition matrix element is calculated on the basis of the diffractive model of Austern and Blair.³ The DWBA parametrization is thus extremely simple and allows very fast computation. The second ingredient of the calculations for the population of the continuum states is the level density of the residual nucleus. This level density can be assumed to be similar to the usual statistical level density.

The main interest of this new formalism is to allow us to distinguish for a surface reaction between a quasielastic transfer process and a process where a large number of degrees of freedom of the projectile and target system are severely relaxed as occurs, for instance, in deep inelastic collisions.⁴ In the distorted wave method formalism, these deep inelastic collisions would be

treated as multistep processes.

Various examples of analysis with this model for several nucleon transfer reactions induced by ¹⁶O on various targets at different incident energies will be presented in order to illustrate the previous point of view.

II. DIFFRACTIONAL MODEL

For a zero spin system, the DWBA cross section for a given transfer angular momentum can be written as

$$\sigma(\theta, E_f, J=L) = \frac{\mu_i \mu_f}{(2\pi \hbar^2)^2} \frac{k_f}{k_i} \sum_M |T_L^M|^2 \tag{1}$$

with

$$T_L^M = \tau_L \frac{4\pi}{k_i k_f} \sum_{i, i'} i^{i-i'} \beta_{i, i'} e^{i(\sigma_i^i + \sigma_i^{i'})} (2L'+1)^{1/2} \times Y_{i'}^M(\theta, 0) \langle l' L - M M | l 0 \rangle \langle l' L 0 0 | l 0 \rangle,$$

where the indices *i* and *f* refer, respectively, to the initial and final channels, μ is the reduced mass and *k* the wave number, and *l* and *l'* are, respectively, the partial wave angular momentum in the entrance and exit channels. The value τ_L is the "transfer parameter." The σ_i are the Coulomb phase shift

$$\sigma_i = \arg \Gamma(l+1+in), \tag{2}$$

where *n* is the Sommerfeld parameter in entrance or exit channel,

$$n = \frac{ZZe^2}{\hbar v}.$$

The two brackets are the usual Clebsch-Gordan coefficients.

In the no-recoil approximation and for quasi-

elastic transfers, the reduced matrix elements $\beta_{i,i'}$ of Eq. (1) are proportional to the product of the derivatives of the reflection coefficient η_i , respectively, in the entrance and exit channels:

$$\beta_{i,i'} = \frac{1}{2i} \left\{ E_i E_{i'} \frac{\partial \eta_i}{\partial l} \frac{\partial \eta_{i'}}{\partial l'} \right\}^{1/2}, \quad (3)$$

where E_i and $E_{i'}$ are, respectively, the center of mass energy in the entrance and exit channels. This formula is just an extension of the Austern-Blair theory for inelastic excitation.³ As expected, the $\beta_{i,i'}$ are then peaked at the nuclear surface.

The Frahn and Venter semiclassical parametrization⁵ is used to describe the coefficient of reflection η_i in the strong absorption model:

$$\eta_i = \{1 + \exp[(l_g - l)/\Delta]\}^{-1}, \quad (4)$$

where the grazing wave l_g and the width Δ are given by the following semiclassical relationships:

$$l_g + kR \left[1 - \frac{2n}{kR} \right]^{1/2}, \quad (5)$$

$$\Delta = kd \left[1 - \frac{n}{kR} \right] \left[1 - \frac{2n}{kR} \right]^{-1/2}, \quad (6)$$

where n is the Sommerfeld parameter and k the wave number. The values R and d are, respectively, the radius and the diffuseness parameters. These parameters are related to those determined from phase shift analysis of the elastic scattering in the entrance and exit channels. The grazing wave l_g and width Δ are obviously different in the entrance and exit channels.

The parametrization of the DWBA cross sections $\sigma(\theta, E_f, J=L)$ of formula (1) can be drastically improved by modifying the Coulomb phase shifts σ_i^i and $\sigma_{i'}^{i'}$. Effectively, the two parameters R and d which allow the calculations of the $\beta_{i,i'}$ through formulas (3)–(6) do not give the possibility of reproducing the shape of the transfer reaction angular distributions. These parameters R and d have to be strongly modified in order to focus the calculated angular distribution to the forward angles where the experimental cross section is peaked. This procedure is similar to the one which consists of modifying the optical model parameters in the entrance and exit channels in the usual DWBA analysis. Even with a strong modification of the radius R , it is, in most of the cases, impossible to obtain the correct shape of the angular distributions. Thus, in order to produce the necessary shift of the calculated angular distribution to the forward angle, we have introduced a nuclear rainbow in the pure Coulomb deflection function for a charged point:

$$\theta_i = 2 \arctan \frac{n}{l}. \quad (7)$$

The new phase shift $\hat{\sigma}_i^{i'}$, used in formula (1), is then parametrized as

$$\hat{\sigma}_i = \sigma_i \left[1 + \exp\left(\frac{l - l_g}{\Delta}\right) \right]^{-1}. \quad (8)$$

The nuclear plus Coulomb deflection function is now

$$\begin{aligned} \hat{\theta}_i &= 2 \frac{\partial \hat{\sigma}_i}{\partial l} \\ &= 2 \arctan \frac{n}{l} - 2\alpha \frac{\partial}{\partial l} \left[1 + \exp\left(\frac{l - l_g}{\Delta}\right) \right]^{-1}. \end{aligned} \quad (9)$$

The value of the nuclear rainbow angle is then

$$\theta_{i=i_g} = 2 \arctan \frac{n}{l_g} - \frac{\alpha}{2\Delta}. \quad (10)$$

This is illustrated in Fig. 1 for the elastic scattering of ^{16}O on ^{54}Fe at 46 MeV incident energy. The quantity $\Delta\theta$ written on Fig. 1 is just $\Delta\theta = -\alpha/2\Delta$. The local minimum (nuclear rainbow) around the grazing wave $l_g = 17$ produces the necessary shift to forward angle of the calculated cross section with formula (1). The cross section is then depending only on three parameters: the radius $R = r_0(A_1^{1/3} + A_2^{1/3})$, the diffusivity d , and the phase angle $\Delta\theta$. The radius r_0 is determined from the elastic scattering—for instance, using the quarter point method of J. S. Blair⁶—and is usually 1.55 fm.

The DWBA cross section $\sigma(\theta, E_f, J=L)$ is maximum for an $L=0$ transfer when the grazing waves are equal in the entrance and exit channels. This allows us to determine the Q value of the reaction for which this condition is fulfilled by eliminating the grazing wave l_g between the center of mass energy equations of the entrance and exit channels:

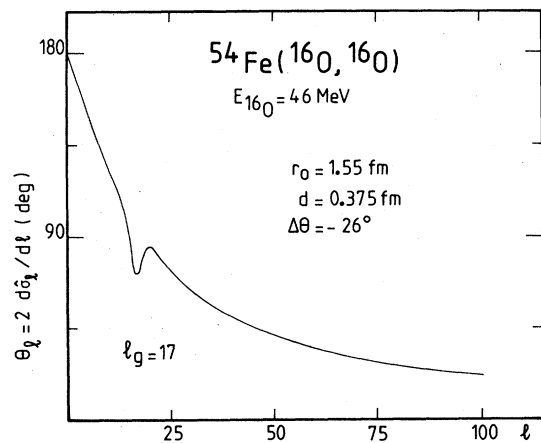


FIG. 1. Deflection function of ^{16}O elastic scattering on ^{54}Fe target [see formula (9) in the text]; $\Delta\theta = -\alpha/2\Delta = -26^\circ$.

$$E_i = V_i^{\text{Coul}} + \frac{\hbar^2}{2\mu_i R_i^2} l_g(l_g + 1)$$

and

$$E_i + Q = V_f^{\text{Coul}} + \frac{\hbar^2}{2\mu_f R_f^2} l_g(l_g + 1).$$

The cross section $\sigma(\theta, E_f, J=0)$ is then maximum for the following Q value:

$$Q_{\text{max}} = -(E_i - V_f^{\text{Coul}}) + \frac{\mu_i R_i^2}{\mu_f R_f^2} (E_i - V_i^{\text{Coul}}). \quad (12)$$

This quantity is very different from the usual optimum Q value quoted in the literature.⁷ The behavior of the cross sections following the excitation energy in the final nucleus is plotted on Fig. 2 for the $^{54}\text{Fe}(^{16}\text{O}, ^{12}\text{C})^{58}\text{Ni}$ four nucleons stripping reaction and for three different values of transfer angular momentum L . The calculations were performed at 56 MeV ^{16}O incident energy. As expected, the cross sections decrease as the excitation energy increases.

III. POPULATION OF THE CONTINUUM STATES

For the quasielastic transfer reactions to the continuum states, the double differential cross section in the center of mass system is given by

$$\frac{d^2\sigma}{d\Omega dE_f} = \sum_J \rho(J, E^*) \sigma(\theta, E_f, J), \quad (13)$$

where $\rho(J, E^*)$ is the level density including the σ^2 spin cutoff term of the residual nucleus:

$$\rho(J, E^*) = (2J+1) e^{-J(J+1)/2\sigma^2} \rho(0, E^*), \quad (14)$$

where $\rho(0, E^*)$ is the density of spin 0 level given, for instance, by the relationships of Gilbert and Cameron⁸:

$$\rho(0, E^*) = \frac{\exp(2\sqrt{aU})}{24\sqrt{2}\sigma^3} \frac{1}{a^{1/4}U^{5/4}}. \quad (15)$$

The various parameters involved in formulas (14) and (15) can be calculated, for instance, by using the table of shell correction energies and pairing energies given in Ref. 8. The quantity U is the excitation energy after subtraction of the proton and neutron pairing energies and a is the level density parameter which is roughly equal to $A/8$ outside the magic nucleus regions where strong deviations are observed.⁹ Let us note that the spin law distribution [formula (14)] is bell shaped and that the most abundant spin at a given excitation energy is $J = \sigma$.

For the sake of simplicity, in our experimental data analysis, a more simple form was preferred for the spin zero level density⁹:

$$\rho(0, E) = \rho_0 \exp(E^*/T), \quad (16)$$

where ρ_0 is a constant and T is the nuclear temperature.

In formula (14) we can consider that the spin cutoff is equal to

$$\sigma^2 = \frac{\mathcal{I}T}{\hbar^2}, \quad (17)$$

where \mathcal{I} is the effective moment of inertia of the nucleus. It is well known that this moment of inertia increases with the excitation energy up to the rigid body value.

Writing formula (13), we have implicitly assumed that the excitation energy of the ejectile can be neglected and that the fragmentation of the projectile does not compete seriously with the transfer mechanism leading to continuum states of the residual nucleus. Furthermore, it is also assumed that the one-step process is the dominant mechanism. Multistep process calculations will lead to description of deep inelastic phenomena and are not presently taken into account.

The double differential cross section $d^2\sigma/d\Omega dE_f$ can be rewritten also as

$$\frac{d^2\sigma}{d\Omega dE_f} = \rho(0, E^*) \sum_J (2J+1) e^{-J(J+1)/2\sigma^2} \sigma(E_f, J). \quad (18)$$

The numerical calculations show that the summation over J is a function exponentially decreasing with the excitation energy while the level density $\rho(0, E^*)$ is exponentially increasing but most of the time with a lower rapidity. That explains the bell-shaped energy spectrum of the heavy ion re-

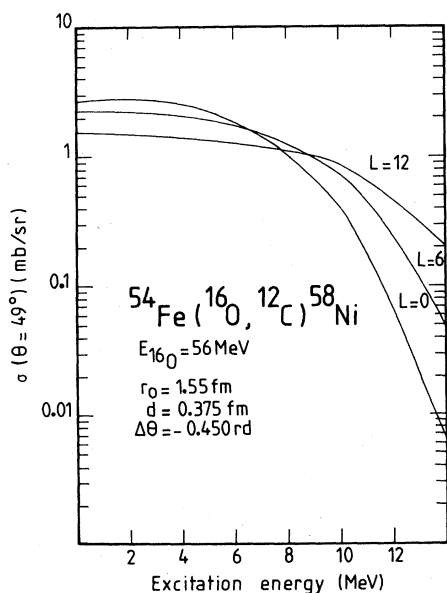


FIG. 2. Theoretical cross section of the $^{54}\text{Fe}(^{16}\text{O}, ^{12}\text{C})^{58}\text{Ni}$ reaction at the grazing angle for various L angular momentum transfer at 56 MeV ^{16}O incident energy.

actions. The rapidity of the exponential decrease of the summation over J is inversely proportional to the value of the diffusivity parameter of the nuclei.

From formula (18) it can be seen that as the excitation energy increases, more higher spin states can be populated. Nevertheless, there is a window spin due to the spin cutoff term. Furthermore, $\sigma(E_f, J)$ decreases as the excitation energy increases (see, for instance, Fig. 2).

From the behavior of the level density $\rho(J, E^*)$ with spin and excitation energy and from the behavior of the DWBA reduced cross section, formula (1), with respect to the Q maximum value, it turns out that in few nucleon stripping reactions, bell-shaped energy spectra are obtained which correspond to population of high spin states for high excitation energy in the final nucleus. Large transfers of nucleons are inhibited due to the Q value mismatch with respect to the Q maximum, formula (12). Furthermore, for these last reactions, the ground states are not populated, because high angular momentum transfers L are required to assure the balance between the entrance channel- and exit channel-grazing waves. The weak point of this transfer reaction model are the transfer parameters τ_L which presently cannot be theoretically calculated. For fitting purposes, τ_L has to be assumed constant and independent of the L transfer for the overall range of excitation energy. This quantity τ_L , in average, is a very small number since we are populating only a given class of states: In fact, the states which have configurations made with the transferred nucleons coupled to the target nucleus on its ground state. We can hope that this class of states has, at high excitation energy, the same kind of spectroscopic factors in average and that their level density is similar to the statistical level density.

IV. RESULTS AND DISCUSSIONS

In all the present analyses the diffractive model parameters—radius $R(r_0)$, diffusivity d , and phase angle $\Delta\theta$ —have been fixed by analyzing the experimental angular distributions of the heavy ion transfer reactions. The radius r_0 was kept constant to 1.55 fm, the usual value for heavy ion elastic scattering.¹⁰ These parameters are the same in the entrance and exit channels.

We shall present first the analysis of the angular distributions of the discrete states of various energy spectra. It is important to show how powerful and accurate is the diffractive model for well known states. This analysis on discrete states allows us to determine the diffractive model parameters used later on in the analysis

of the continuum spectra. The free parameters for this second analysis being ρ_0 , σ^2 , and T in formula (13).

A small computer code named FAST has been written to calculate the reduced differential cross sections for different L transfer and final energies which are stored on magnetic disc and used in a second step by an automatic search code FITS to determine the level density parameters ρ_0 , T , and σ^2 which allow us to reproduce the experimental shape of excitation energy spectra.

A. The four-nucleon stripping reaction: $^{54}\text{Fe}(^{16}\text{O}, ^{12}\text{C})^{58}\text{Ni}$

For the reaction $^{54}\text{Fe}(^{16}\text{O}, ^{12}\text{C})^{58}\text{Ni}$ the angular distributions for the discrete levels and the energy spectrum have been measured, respectively, at 46 and 56 MeV ^{16}O incident energy.¹¹ All the angular distributions have the same bell-shaped pattern independently of the final level reached by the transfer reaction. In Fig. 3 the 1.45 MeV 2^+ state angular distribution of the ^{58}Ni final nucleus is presented. This fit has been obtained with formula (1). The diffractive parameters are given in Table I: family II. The phase angle was adjusted in order to reproduce the experimental points: $\Delta\theta = -0.450$ rad (or -26°). The diffusivity parameter d is responsible for the width of the experimental angular distribution. The

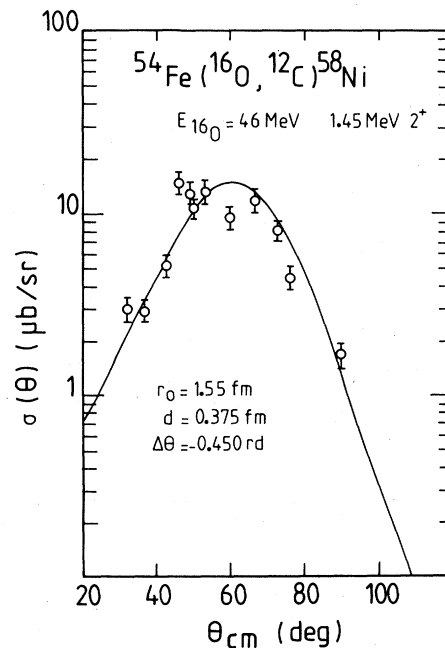


FIG. 3. Angular distribution of the $^{54}\text{Fe}(^{16}\text{O}, ^{12}\text{C})^{58}\text{Ni}$ reaction of the first 2^+ level of ^{58}Ni measured at 46 MeV ^{16}O incident energy. The theoretical curve has been obtained with the diffractive model [formula (1)].

TABLE I. Diffractive model parameters.

System	Incident energy (MeV)	r_0 (fm)	d (fm)	Δ (rad)	D.M. ^a family
$^{54}\text{Fe} + ^{16}\text{O}$	46	1.90	0.375	0	I
		1.55	0.375	-0.450	II
$^{64}\text{Ni} + ^{16}\text{O}$	56	1.60	0.250	-0.750	I
$^{48}\text{Ca} + ^{16}\text{O}$	59.5	1.55	0.375	-0.600	I
$^{76}\text{Ge} + ^{16}\text{O}$	56	1.55	0.375	-0.500	I
		1.90	0.375	0	II
$^{208}\text{Pb} + ^{16}\text{O}$	140 - 312	1.55	0.550	-0.050	I
		1.55	0.300	-0.250	II

^aDiffractive model family.

width of the calculated curve varies inversely proportional to d . If no phase angle is used ($\theta\Delta=0$), which means that pure Coulomb phase shifts are used in formula (1), to calculate the transfer cross section the same bell-shaped curve is obtained but centered 20° at a more backward angle. In this particular case a correct calculated angular distribution centered at 60° can also be obtained with pure Coulomb phase shift ($\Delta\theta=0^\circ$) if we used a reduced radius $r_0=1.90$ fm instead of 1.55 fm given by elastic scattering phase shift analyses.¹⁰ This new set of parameters is called family I in Table I. Thus, there is no ambiguity in the determination of the diffractive model parameters.

B. The two-proton stripping reaction: $^{64}\text{Ni}(^{16}\text{O},^{14}\text{C})^{66}\text{Zn}$,
 $^{48}\text{Ca}(^{16}\text{O},^{14}\text{C})^{50}\text{Ti}$, and $^{76}\text{Ge}(^{16}\text{O},^{14}\text{C})^{78}\text{Se}$

The ($^{16}\text{O},^{14}\text{C}$) angular distributions measured at 56 MeV ^{16}O incident energy on a ^{64}Ni target nucleus are presented in Fig. 4 and are well fitted by the diffractive model.¹² The experimental L dependence of the differential cross sections are well reproduced by the model. It can be noted that oscillations disappear for high L transfer and for poor Q matched reactions. The radius $r_0=1.60$ fm is unusually large. This is due to the necessity to reproduce perfectly, in phase, the experimental oscillations of the angular distributions. The diffractive model parameters extracted from this fitting procedure are listed on Table I. The transfer parameter τ_L^2 are, respectively, for the ground state, first 2^+ state, and first 3^- state: 0.087, 0.11, and 0.46. No continuum energy spectrum is observed at this low incident energy in this reaction due to the large negative Q value ($Q_{\text{g.s.} \rightarrow \text{g.s.}} = -5.971$ MeV).

A similar analysis to the one performed for the ($^{16}\text{O},^{14}\text{C}$) reaction on ^{64}Ni was done for the ^{48}Ca

($^{16}\text{O},^{14}\text{C}$) ^{50}Ti two-proton stripping reaction studied at 59.5 MeV ^{16}O incident energy.¹³ The diffractive model parameters are given in Table I, the phase angle is $\Delta\theta=-0.60$ rad. It is completely impossible to obtain correct fits with pure Coulomb phase shift ($\Delta\theta=0$) by manipulating only the radius and the diffusivity parameters. Two typical angular distributions are displayed in Fig. 5 for the ground state and 3.20 MeV 6^+ levels of ^{50}Ti . The normalization factors τ^2 are, respectively, 13.9 and 5.2 in arbitrary units since the experimental cross sections are unknown in absolute values for this experiment.

In Fig. 6 various fits on the first levels of ^{78}Se , reached by the ($^{16}\text{O},^{14}\text{C}$) transfer reaction on ^{76}Ge , are presented.¹⁴ Two-step processes involving target core excitation have been previously evidenced for this kind of reaction, in particular for the first 2^+ level of ^{78}Se at 0.613 MeV excitation energy.¹⁴ The 0^+ ground state and 2.50 MeV 3^- are mainly populated by one-step processes and the corresponding diffractive model parameters providing perfect fits with formula (1) are, respectively, $r_0=1.55$ fm, $d=0.375$ fm, and $\Delta\theta=-0.50$ rad. On the other hand, with these parameters, the calculated angular distribution of the first 2^+ level is also bell-shaped while the experimental angular distribution is oscillating and strongly peaked at forward angles. It is well known that the transition matrix elements in the l space for indirect route are much narrower than the one corresponding to direct route. Furthermore, the deflection function for the indirect route is also much more peaked to the forward angle than the deflection function of the direct route.¹ Effectively, the dashed curve of the 0.613 MeV 2^+ level was obtained with the following parameters: $r_0=1.55$ fm, $d=0.200$ fm, and $\Delta\theta=-0.750$ rad. The normalization factors τ_L^2 for the ground state, the 0.613 MeV 2^+ , and 2.50 MeV 3^- are, respectively, 0.0526, 0.010, and 0.049.

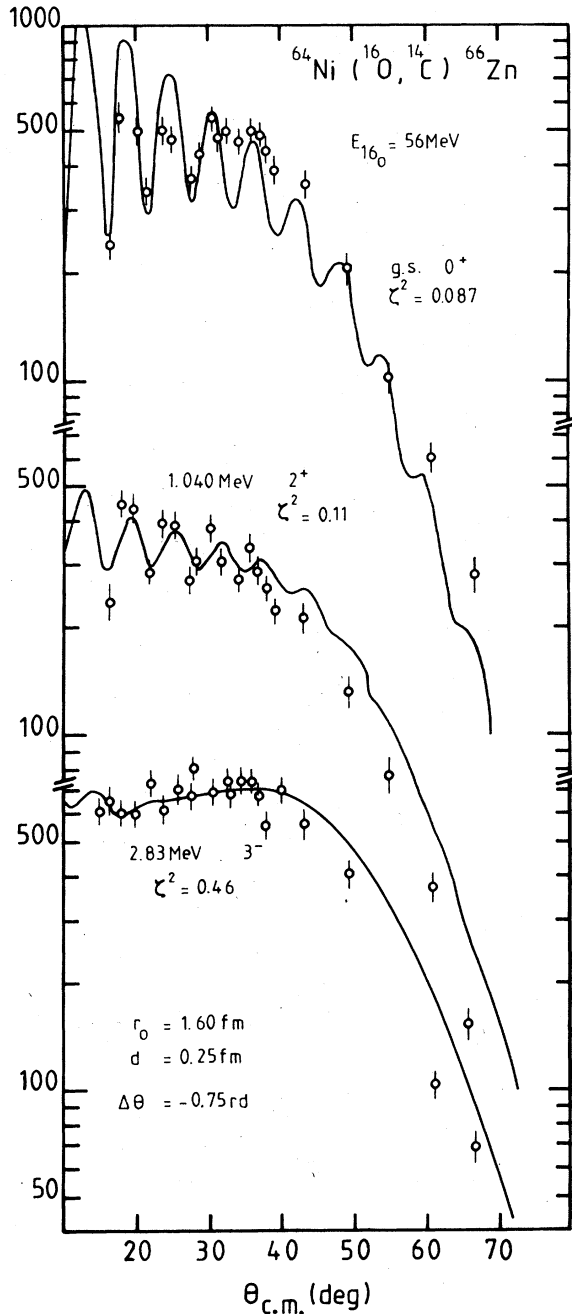


FIG. 4. Angular distributions of the $^{64}\text{Ni}(^{16}\text{O}, ^{14}\text{C})^{66}\text{Zn}$ two-proton transfer reaction measured at 56 MeV ^{16}O incident energy for the first few excited states.

C. The one-proton transfer reaction induced by ^{16}O on ^{208}Pb target

The ground state angular distributions of the $(^{16}\text{O}, ^{15}\text{N})$ reaction on the ^{208}Pb target¹⁵ are fitted by the diffractive model for several incident energies: 104, 140, 216.6, and 312 MeV. The theoretical curves of Fig. 7 were obtained with a

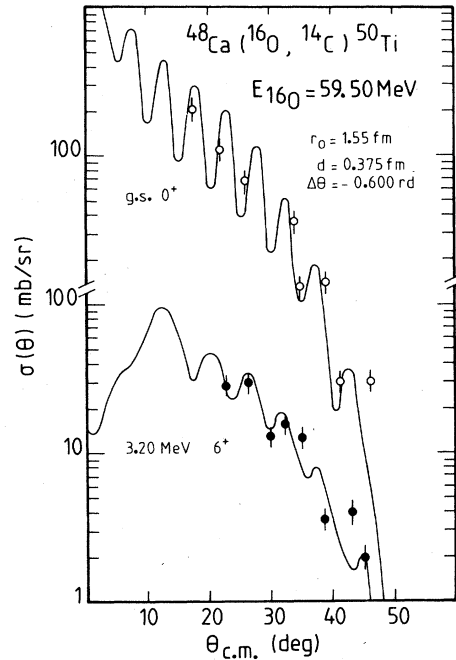


FIG. 5. Angular distributions of the $^{48}\text{Ca}(^{16}\text{O}, ^{14}\text{C})^{50}\text{Ti}$ reaction measured at 59.50 MeV ^{16}O incident energy for the ground state and first 6^+ level of ^{50}Ti . The theoretical curves are obtained with the diffractive model [formula (1)] and with the modified Coulomb phase shifts.

unique family of diffractive model parameters for the four different energies. These parameters are listed in Table I: family I. The corresponding τ_L^2 transfer parameters for this $h_{9/2}$ - $L=5$ transition are listed in Table II. This parameter τ_L^2 decreases regularly as the ^{16}O incident energy increases. The same behavior with the same order of discrepancy was observed previously in a standard DWBA analysis taking into account the recoil effects by the authors of Ref. 15. The theoretical cross section increases faster than the experimental one with the incident energy in both types of DWBA calculations.

D. Transfer reactions to the continuum states

Figure 8 presents the ^{12}C energy spectrum of the $^{54}\text{Fe}(^{16}\text{O}, ^{12}\text{C})^{58}\text{Ni}$ four-nucleon transfer reaction measured at 56 MeV and at the grazing angle 40° .¹¹ The solid curve corresponds to the use of pure Coulomb phase shifts in the DWBA calculation; see formulas (1) and (2). The parameters are listed as family I in Table I. On the other hand, the dashed curve has been obtained with the parameter of family II and corresponds to the use of Coulomb plus nuclear phase shifts; see formulas (1), (2), and (8) in Table III. The quantity χ^2 is defined as

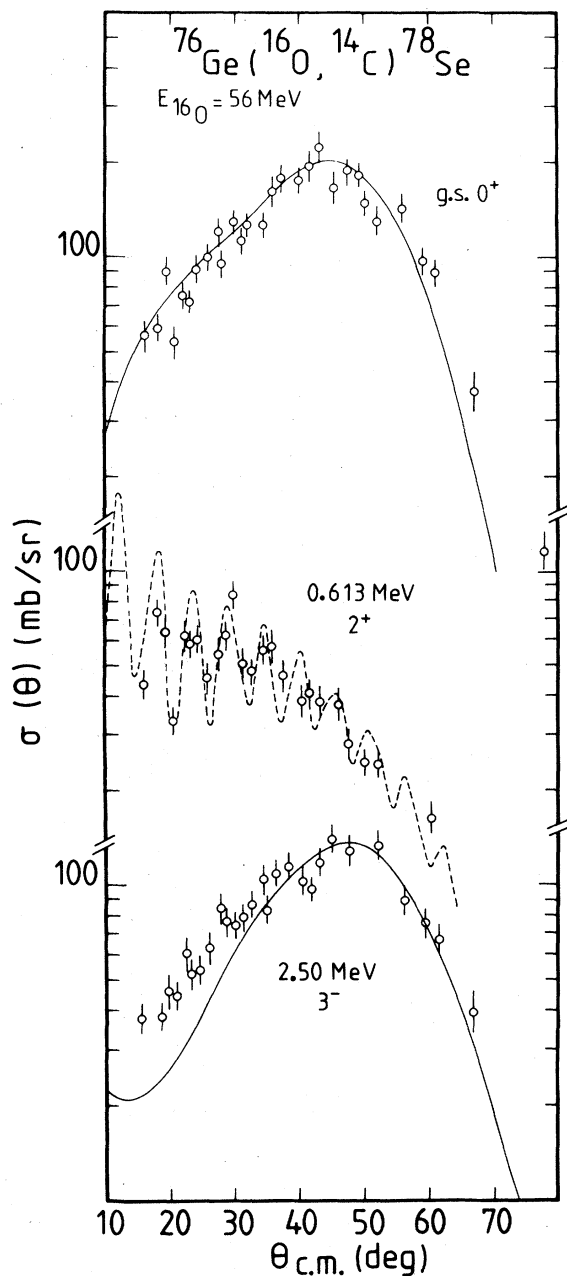


FIG. 6. Angular distributions of the $^{76}\text{Ge}(^{16}\text{O}, ^{14}\text{C})^{78}\text{Se}$ reaction for the first few excited levels of ^{78}Se . The curves are obtained from the diffractive model (see text).

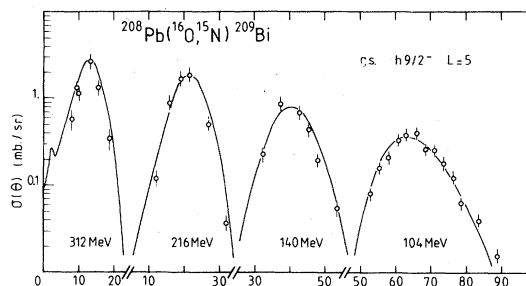


FIG. 7. Ground state angular distributions of the $^{208}\text{Pb}(^{16}\text{O}, ^{15}\text{N})^{209}\text{Bi}$ one-proton transfer reaction measured at several ^{16}O incident energies.

$$\chi^2 = \frac{1}{N} \sum_{i=1}^N (\sigma_{\text{exp}}^i - \sigma_{\text{theo}}^i)^2,$$

where N is the number of experimental points which define the average shape of the energy spectrum. The χ^2 is given in arbitrary units.

The quality of both fits is presently similar. The level density parameters T , \mathcal{J}/\hbar^2 , or σ^2 extracted from this automatic search analysis are given in Table III. The level densities are not determined in all these analyses in absolute values since the transfer parameter τ_L^2 is unknown and assumed constant and independent of the L transfer. There is a certain ambiguity between the temperature T and the spin cutoff term σ^2 or the moment of inertia $\mathcal{J}(\sigma^2 = \mathcal{J}T/\hbar^2)$. Equally good fits can be obtained with different combinations of these two parameters. In Table III, the quantity labeled T_0 is the statistical level density temperature calculated at the centroid energy of the spectrum according to the systematics of Gilbert and Cameron⁸ and also of Baba,¹⁰ the quantity \mathcal{J}_0 is the rigid body moment of inertia for a spherical nucleus, and σ_0^2 is the spin cutoff parameter for the statistical level density according to the systematics of Gilbert and Cameron.⁸ Since the temperature T determined in the present analysis is higher than the one of the statistical level density, the moment of inertia \mathcal{J} is then much lower than the rigid body value \mathcal{J}_0 , which is any way an upper limit. On the other hand, the quantity σ^2 is of the same order of magnitude as the σ_0^2 of Gilbert and Cameron⁸ (statistical level density).

TABLE II. Transfer parameter τ_L^2 for $^{208}\text{Pb}(^{16}\text{O}, ^{15}\text{N})^{209}\text{Bi}$ ($h_{9/2-}$, g.s.).

Incident energy (MeV)	104	140	216.6	312
$\tau_L^2 = 5$	0.114	0.0909	0.0562	0.0375

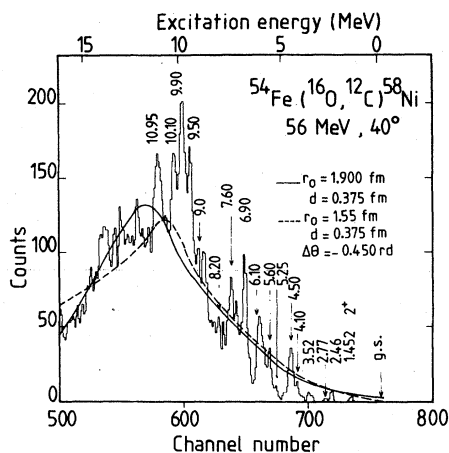


FIG. 8. Energy spectrum of the $^{54}\text{Fe}(^{16}\text{O}, ^{12}\text{C})^{58}\text{Ni}$ reaction measured at 56 MeV ^{16}O incident energy and 40° lab. The two curves were obtained with the diffractive model for two different sets of parameters. The dashed curve corresponds to modified Coulomb phase shifts [see formula (9)].

Figure 9 presents the ^{14}C energy spectrum of the $^{48}\text{Ca}(^{16}\text{O}, ^{14}\text{C})^{50}\text{Ti}$ two-proton transfer reaction measured at 59.5 MeV excitation energy and at 17° laboratory angle.¹³ The fit is excellent and the corresponding parameters of the level density are given in Table III. The drawn curve has a $\chi^2=40$. In this analysis the temperature is also higher than the one of the statistical level density.

A similar example is given for the $(^{16}\text{O}, ^{14}\text{C})$ two-proton transfer reaction on ^{76}Ge target nucleus measured at 56 MeV ^{16}O incident energy and 20° laboratory angle.¹⁴ The best fit, solid curve of

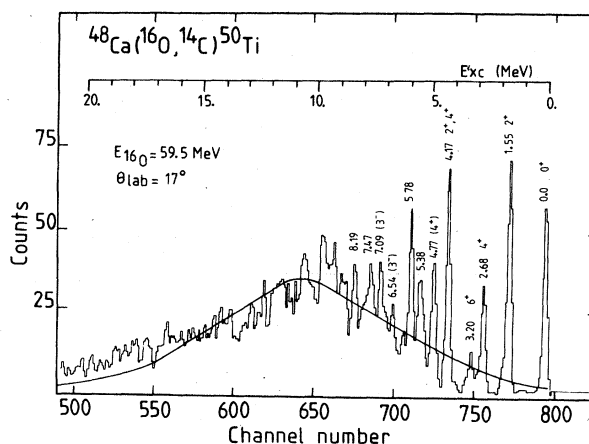


FIG. 9. Energy spectrum of the $^{48}\text{Ca}(^{16}\text{O}, ^{14}\text{C})^{50}\text{Ti}$ reaction measured at 17° lab and 59.5 MeV ^{16}O incident energy. The solid line is a result of a best fit using the diffractive model.

Fig. 10, corresponds to the use of pure Coulomb phase shift in the DWBA calculations, family II of Table I. The dashed curve, on the other hand, corresponds to family I for the diffractive model parameters ($\chi^2=262$). The nuclear phase shift is then taken into account. As in the previous analysis, the temperature T is much higher than the statistical one T_0 .

The ^{12}C and ^{11}B spectra¹⁷ obtained by bombarding the ^{208}Pb target with an 140 MeV ^{16}O beam were analyzed in the same vein. Figure 11 presents the ^{12}C and ^{11}B spectra measured at the grazing angle: 40° lab. The diffractive model para-

TABLE III. Level density parameters.

Nucleus	T (MeV)	J/\hbar^2 (MeV $^{-1}$)	σ^2	Spectrum centroid				χ^2 a.u.	D.M. family
				energy (MeV)	T_0 (MeV)	\mathcal{J}_0 (MeV $^{-1}$)	σ_0^2		
^{58}Ni	1.752	5.50	9.64	11	1.253	11.90	9.06	316	II
	1.766	5.50	9.72					72	I
	1.831	6.50	11.90					74	I
^{50}Ti	2.782	4.10	11.41	9	0.929	9.29	7.56	64	I
	3.171	5.50	17.44					40	I
^{78}Se	1.434	6.50	9.32	7	0.663	19.50	11.50	263	I
	1.612	8.50	13.70					262	I
	1.356	8.50	11.53					121	II
^{212}Po (140 MeV)	4.132	15.96	65.94	25	1.531	103.26	62.85	504	II
	3.062	10.34	31.66					636	II
^{212}Po (312 MeV)	8.788	1.92	16.87					59	II
^{213}At (140 MeV)	3.126	15.0	44.89	25	1.559	104.07	67.67	812	II
	3.320	20.0	66.4					483	II
	3.320	23.80	79.02					361	II

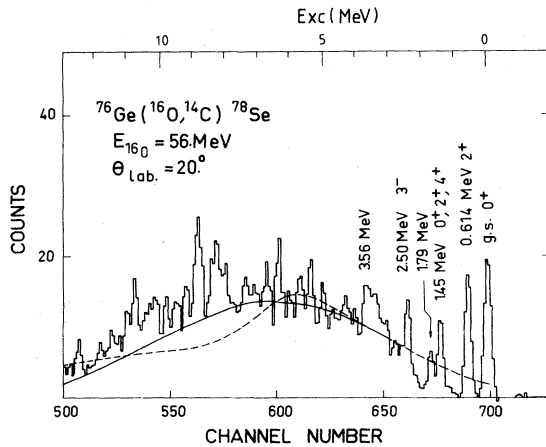


FIG. 10. Experimental energy spectrum of the ^{76}Ge - $(^{16}\text{O}, ^{14}\text{C})^{78}\text{Se}$ reaction measured at 56 MeV ^{16}O incident energy and 20° lab. The solid curve corresponds to pure Coulomb phase shift in the diffrational model while for the dashed curve nuclear phase shifts were taken into account.

eters are those of family II of Table I. They were obtained by analyzing the one-proton transfer reactions on the ^{208}Pb target for highly excited states of ^{209}Bi .¹⁷ The corresponding level density parameters are given in Table III. The drawn curves are for a χ^2 of 504 for the ^{12}C case and for a χ^2 of 483 for the ^{11}B case. The temperature T is still too high by a factor of 2 with respect to the statistical one T_0 . On the other hand, the spin cutoff parameter σ^2 is very close to the statistical limit σ_0^2 as in the previous examples.

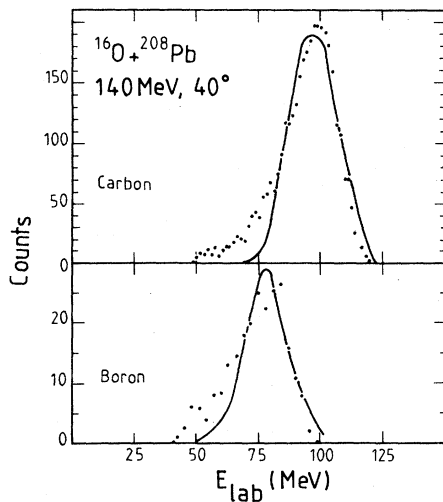


FIG. 11. Experimental energy spectra of the $(^{16}\text{O}, ^{12}\text{C})$ and $(^{16}\text{O}, ^{11}\text{B})$ reactions on ^{208}Pb target nucleus measured at 140 MeV ^{16}O incident energy. The solid curve is a best fit obtained from the diffrational model.

The spectra obtained at high incident energy, namely 312 MeV of ^{16}O , cannot be fitted with reasonable parameters. The temperature T and spin cutoff term σ^2 are, respectively, 8.8 MeV and 17. The best fit obtained with these parameters is presented in Fig. 12. It has been shown that at 20 MeV/nucleon the reaction mechanism is not any more of a quasielastic type but more likely a fragmentation process.¹⁷ It is probably for this reason that we have obtained the level density parameters corresponding to a very light nucleus. Lukyanov and Titov¹⁸ had established that the integrated cross section on energy for a fragmentation process is roughly proportional to the level density of the ejectile multiplied by a dynamical factor taking into account the Q matching of the fragmentation reaction.

V. SUMMARY

It has turned out that the diffrational model, using modified Coulomb phase shift, is very successful in accounting for the transfer reaction angular distributions of discrete levels. As expected, for levels populated mainly by two-step processes the diffusivity parameter has to be much smaller than in case of a one-step process and the phase angle has to be also much larger, which means that the deflection function is more peaked at forward angles.

As far as continuum states are concerned, very reasonable fits can be obtained; nevertheless, a serious discrepancy is present concerning the level density temperature. The temperatures found in this analysis are different from the statistical one but are of the same order of magnitude than the ones given by a Volkov plot for a $Q_{g.s.} - g.s.$ systematics.¹⁶ On the other hand, the spin cutoff values σ^2 agree rather well with the systematics of Gilbert and Cameron for statistical level densities.⁸

The complete failure of the model at very high ^{16}O incident energy on ^{208}Pb target is due to the

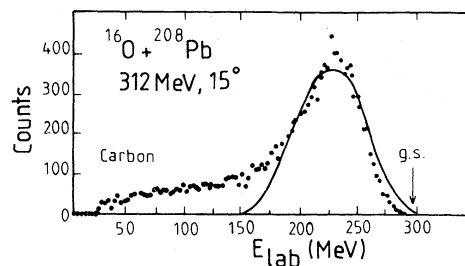


FIG. 12. Experimental energy spectrum of the $(^{16}\text{O}, ^{12}\text{C})$ reaction on ^{208}Pb target nucleus measured at 312 MeV ^{16}O incident energy. The solid curve is a best fit using the diffrational model.

fact that we are dealing with fragmentation processes of the projectile instead of pure direct transfer reaction.

The fact that some spectra can be fitted up to the Coulomb barrier of the ejectile is in favor of the wide excitation energy range of quasielastic transfer reactions. On the other hand, it would be impossible, with this one-step model of direct surface reaction, to reproduce the second bump

observed in some spectrum in the vicinity of the Coulomb barrier of the ejectile.⁴ This second bump corresponds effectively to deep inelastic collisions or, in other words, to multistep processes.

Sincere thanks are due to Dr. B. T. Kim and Dr. J. Raynal for useful discussions concerning the coding of the formulas contained in this article.

-
- ¹K. S. Low, *J. Phys. (Paris), Colloq.* **37**, C5 (1976); T. Udagawa, in *Proceedings of the International Conference on Nuclear Structure, Tokyo, 1977*, edited by T. Marumori (Physical Society of Japan, Tokyo, 1978), Vol. 44, suppl. 667; N. K. Glendenning, in *Proceedings of the International Conference on Reactions between Complex Nuclei, 1974*, edited by R. L. Robinson, F. K. Mc Govan, J. B. Ball, and J. H. Hamilton (North-Holland, Amsterdam, 1974), p. 137; R. J. Ascutto and J. S. Vaagen, *ibid.*, p. 257.
- ²T. Udagawa, T. Tamura, and B. T. Kim, *Phys. Lett.* **82B**, 349 (1979); T. Udagawa and T. Tamura, *Phys. Rev. Lett.* **41**, 1770 (1978); H. Fröhlich, T. Shimoda, M. Ishihara, K. Nagatani, T. Udagawa, and T. Tamura, *ibid.* **42**, 1518 (1979).
- ³N. Austern and J. S. Blair, *Ann. Phys. (N.Y.)* **33**, 15 (1965); F. J. W. Hahne, *Nucl. Phys.* **A104**, 545 (1967).
- ⁴V. V. Volkov, *Phys. Rep.* **44**, 93 (1978); M. Lefort and Ch. Ngô, *Ann. Phys. (N.Y.)* **3**, 5 (1978).
- ⁵W. E. Frahn and R. H. Venter, *Ann. Phys. (N.Y.)* **24**, 243 (1963); *Nucl. Phys.* **59**, 651 (1964).
- ⁶J. S. Blair, *Phys. Rev.* **95**, 1218 (1954).
- ⁷J. P. Schiffer, H. J. Körner, R. H. Siemssen, K. W. Jones, and A. Schwarzschild, *Phys. Lett.* **44B**, 47 (1973).
- ⁸A. Gilbert and A. G. W. Cameron, *Can. J. Phys.* **43**, 1446 (1965).
- ⁹J. R. Huizenga and L. G. Moretto, *Annu. Rev. Nucl. Sci.* **22**, 427 (1972).
- ¹⁰P. Bonche, B. Giraud, A. Cunsolo, M.-C. Lemaire, M. C. Mermaz, and J. L. Québert, *Phys. Rev. C* **6**, 577 (1972).
- ¹¹M.-C. Lemaire, *Phys. Rep.* **7**, 279 (1973); H. Faraggi, A. Jaffrin, M.-C. Lemaire, M.-C. Mermaz, J. C. Faivre, J. C. Gastebois, B. G. Harvey, J. M. Loiseaux, and A. Papineau, *Ann. Phys. (N.Y.)* **66**, 905 (1971).
- ¹²M.-C. Lemaire, M.-C. Mermaz, H. Sztark, and A. Cunsolo, *Phys. Rev. C* **10**, 1103 (1974).
- ¹³P. Bonche, ANL Report No. PHY-1973B, 1973, p. 235.
- ¹⁴M. Cobern, M.-C. Lemaire, K. S. Low, M.-C. Mermaz, H. Sztark, T. Udagawa, and T. Tamura, *Phys. Rev. C* **13**, 1200 (1976).
- ¹⁵C. Olmer, M. Mermaz, M. Buenerd, C. K. Gelbke, D. L. Hendrie, J. Mahoney, D. K. Scott, M. H. Macfarlane, and S. C. Pieper, *Phys. Rev. C* **18**, 205 (1978).
- ¹⁶H. Baba, *Nucl. Phys.* **A159**, 625 (1970).
- ¹⁷C. K. Gelbke, C. Olmer, M. Buenerd, D. L. Hendrie, J. Mahoney, M.-C. Mermaz, and D. K. Scott, *Phys. Rep.* **42**, 312 (1978).
- ¹⁸V. K. Lukyanov and A. I. Titov, *Phys. Lett.* **57B**, 10 (1975).